4.2.3.8 Magnetic fields

TILMAN SPOHN

Magnetic fields of internal origin are characteristic of planets and satellites (for a recent review see [07Con]). Magnetized meteorites suggest that even planetesimals may have had their own self-generated fields [08Wei]. In addition to Earth, Mercury, the giant planets Jupiter, Saturn, Uranus, and Neptun, and the Jovian satellite Ganymede are known to have largely dipolar internally generated magnetic fields. Mars has a remnantly magnetized crust in mostly the southern hemisphere [98Acu]. This remnant magnetization is evidence of an earlier self generated field [04Con]. The Moon also has crust units with remnant magnetization located suspiciously close to the antipodes of major impact basins [07Mit]. While the magnetization may be taken as evidence of an ancient magnetic field for the Moon, alternative explanations have been given. One of the alternative explanations invokes plasma generated upon impact where the great basins are formed. Arguments against an early dynamo for the Moon use the small size of its core and its low rotation rate [75Run]. However, recent scaling laws for the dynamos do not invoke the planetary rotation rate but do invoke the size of the core. It has been predicted that Venus should have had an early magnetic field, too [83Ste]. The high surface temperature would have annealed any remnant magnetization since the temperature is above the Curie temperature (the magnetic blocking temperature) of most remanently magnetisable minerals.

4.2.3.8.1 Dynamos

Generation of a magnetic field requires an electrically conducting shell within a planet and motion within that shell. In the terrestrial planets and the satellites this region is believed to be the fluid iron-rich core at the centre. (For recent reviews of Earth and planetary dynamos and convection in the core see [07Rob], [07Chr], [07Jon] and [07Bus].) There may be a solid inner core (see Sections 4.2.3.2 and 4.2.3.4), the growth of which may provide a buoyancy flux that may drive the dynamo. The buoyancy in this case derives from a difference in composition between the solid inner core and the fluid outer core. Light alloying elements such as sulphur and oxygen tend to be expelled from the solidifying core and concentrate in the fluid outer core. In addition to a chemical buoyancy flux from the inner core thermal buoyancy may drive the flow. The thermal buoyancy results from a sufficiently large temperature difference between the core and the rocky mantle surrounding the core. Convection in the core can be described by the field equations of fluid dynamics introduced in Section 4.2.3.4. However, because the viscosity of the iron liquid in the core is many (about 20) orders of magnitude smaller than that of the mantle, inertia and Coriolis forces are important. Because of the magnetic field and the electrical conductivity, the Lorentz force has to be included. The momentum equation then is

$$\rho \left(\frac{\partial}{\partial t} + \boldsymbol{v} \cdot \nabla \right) \boldsymbol{v} + 2\rho \boldsymbol{\Omega} \times \boldsymbol{v} = \nabla p + \rho \boldsymbol{g} + \boldsymbol{j} \times \boldsymbol{B} + \rho \boldsymbol{F} \tag{1}$$

In equ (1), t denotes time, $\boldsymbol{v}$ is the fluid velocity, ρ is the core density, $\boldsymbol{\Omega}$ is the planet's rotation vector, $\boldsymbol{g}$ is the gravity, $\boldsymbol{j}$ is the electric current density, $\boldsymbol{B}$ is the magnetic induction vector, and $\boldsymbol{F}$ is the specific body force (buoyancy). Vector quantities are written in bold face. The first term on the left hand side is the inertia term, the second term denotes the Coriolis force. The third term on the right hand side is the Lorentz force where $\mu j = \nabla \times B$, with μ the magnetic permeability. The equation is supplemented by a conservation of mass equation which in the case of an incompressible fluid reads

$$\nabla \cdot \boldsymbol{v} = 0 \tag{2}$$

and the conservation of entropy equation

$$\rho T \left(\frac{\partial}{\partial t} + \boldsymbol{v} \cdot \nabla \right) S = \nabla \cdot \left(k \nabla T \right) + H \rho \tag{3}$$

where T is temperature, S is entropy, k is the thermal conductivity, and H the rate of release of energy in the core per unit mass, e.g. radiogenic heat production. The equations must be supplemented by an equation of state. Usually, taking the Boussinesq-approximation, the fluid is taken to be incompressible except for the body force where thermal expansion and/or chemical density differences are taken into account.

The magnetic induction equation (written in a simplified form assuming a solenoidal velocity field and a constant magnetic diffusivity λ) is

$$\left(\frac{\partial}{\partial t} + \boldsymbol{v} \cdot \nabla \right) \boldsymbol{B} - \lambda \nabla^2 \boldsymbol{B} = \boldsymbol{B} \cdot \nabla \boldsymbol{v} \tag{4}$$

A sustained magnetic field can be generated by the flow if the production of field energy by the stretching of field lines (the term on the right-hand-side) overcomes the magnetic diffusion on the left hand side. The relative weight of the two terms is measured by the magnetic Reynolds number

$$R_m \equiv \frac{U d}{\lambda} \tag{5}$$

where U is a characteristic velocity and d a characteristic length (e.g., the core radius). The magnetic Reynolds number must be larger than 1 for the dynamo to operate. Other dimensionless parameter groups of relevance to the dynamo problem are the Rayleigh number

$$Ra \equiv \frac{\alpha g \Delta T d^3}{\kappa \nu} \tag{6}$$

where α is the volumetric thermal expansion coefficient, ΔT is the non-adiabatic temperature difference across the convecting layer, κ is the thermal diffusivity, and ν is the kinematic viscosity and the Ekman number

$$E \equiv \frac{\nu}{\Omega d^2} \tag{7}$$

The Rayleigh number measures the vigour of the convection while the Ekman number measures the importance of the Coriolis force. Numerical models of the dynamo driven by a buoyancy flux from below (a growing inner core) have been successful but the models are still far from realistic values of both the Ekman and Rayleigh numbers. Nevertheless, a scaling law has been derived for the magnetic field strength at the surface of the dynamo region [06Chr]

$$B \approx 0.9 \mu^{1/2} \rho^{1/6} \left(\frac{g Q_B d}{4 \pi R_c R_i} \right)^{1/3} \tag{8}$$

where Q_B is the buoyancy flux into the dynamo region (thermal and/or chemical), and R_c and R_i are the outer and inner radii of the core shell. The characteristic length d here is the thickness of the core shell $R_c - R_i$. In this scaling, the magnetic field strength depends on the size of the core and the buoyancy flux but is independent of the electrical conductivity and of the rotation rate although it is still required that the magnetic Reynolds number be larger than 1 and that in order to obtain a dipolar field the Coriolis force must dominate over inertia. (The latter requirement is consistent with the Cowlings theorem, see [07Rob].) The scaling supersedes an older scaling law that was derived from a balance between the Lorentz force and the Coriolis force. In this often used scaling, the magnetic field was proportional to the planetary rotation rate.

As Equ. (8) shows, the magnetic field strength is strongly affected by the heat transfer through the mantle of the planet. The buoyancy flux is directly related to the heat flow extracted by the mantle from

the core for a thermally driven dynamo. For a chemically driven dynamo the rate of inner core growth and therefore the rate of buoyancy release depend on the core cooling rate and therefore on the heat flow from the core. The heat flow from the core can be calculated from planet thermal history models (see Section 4.2.3.4 and [07Bre]),

4.2.3.8.2 Magnetic fields of the terrestrial planets and satellites

The magnetic field strength is measured in Teslas (T). An often used unit in geophysics and planetary science is the Gauss (G) equal to 10^{-4} T. Fields measured by spacecraft close to the planets depend on the orbital distance but typically range from tens of nT (Mercury, Mars) to a few G for Jupiter [07Con]. The measurement of the internal field is perturbed however, by the ambient (external) magnetic field, mostly due to the solar wind but also due to the field of the planet (e.g., Jupiter) if the field of a satellite (e.g., Ganymede) is to be measured. The Earth's surface magnetic field is about 30,000 nT.

The simplest means of characterizing a planetary magnetic field is by fitting a dipole field to the data measured by spacecraft. The dipole can be tilted with respect to the planetary rotation axis and offset from the centre. The model is known as the offset tilted dipole or OTD. The magnetic induction vector $\boldsymbol{B}$ of a dipole is related to the dipole moment $\boldsymbol{m}$ measured in Tm^3 and the radial distance from the centre $\boldsymbol{r}$ by

$$\boldsymbol{B}(\boldsymbol{r}) = -\frac{\boldsymbol{m}}{r^3} + \frac{3(\boldsymbol{m}\cdot\boldsymbol{r})\boldsymbol{r}}{r^5} \tag{9}$$

More complex planetary magnetic fields – such as those of the giant planets – can be modelled by superposing usually a small number of dipoles with differing tilts and moments (compare Section 4.2.4.5). Crustal fields such as the present field of Mars are modelled by using large numbers of dipoles e.g., [00Pur]. In the absence of local currents ($\nabla \times \boldsymbol{B} = \boldsymbol{0}$) the magnetic induction vector $\boldsymbol{B}$ can be expressed as the gradient of a scalar potential that will satisfy the Laplace equation. The potential can be expanded in spherical harmonics and the components of the field can be calculated from the gradient of the potential (see Section 4.2.4.5).

4.2.3.8.2.1 Mercury

The magnetic field of Mercury was detected by the Mariner mission in 1974 [74Nes]. Unfortunately, the field to date has been recorded by four fly-bys only: two passes by Mariner 10 and another two passes by Messenger. Messenger, however, will measure the field much more accurately after it goes into orbit in 2011. The situation will improve even further if the European BepiColombo project will succeed in getting two spacecraft into orbit around the planet. Magnetometers on both spacecraft will allow separating internal from external fields. The mission is planned to be launched in 2014 and orbit insertion is planned for 2020.

The presently available data for Mercury interpreted together suggest a dipole tilted by 5° to 12° with a moment of 230 to 290 nT$\cdot R_M^3$, but non-dipolar terms are found to be significant [09Uno]. These could indicate crustal fields or significant dynamo action close to the core/mantle boundary which should be close to 0.8 R_M. The quality of the data do not yet allow to distinguish between thin shell dynamo models for Mercury ($(R_c - R_i) << R_c$) [04Sta] predicting relatively large non-dipolar terms and thick shell dynamo models ($R_c >> R_i$) [06Chr].

4.2.3.8.2.2 Venus

Missions to Venus have failed to detect a magnetic field of the planet. An upper limit for its dipole moment is 10^{-5} times the moment of the Earth [87PHI] or 0.35 nT·R_V^3. It is concluded that the planet has neither a significant dynamo magnetic field nor a remnant magnetic field. Models of the magnetic history of Venus [83Ste] suggest that Venus may have had an early magnetic field for a few billion years. The field may have failed to produce remnant magnetization because the temperature of crustal rock remained above the Curie temperature of magnetisable minerals.

4.2.3.8.2.3 Mars

Early magnetic field observations at Mars by the US mission Mariner 4 and the Sowjet Phobos 2 mission were inconclusive with regard to the existence of a small dipole field or the absence of the latter [89Rie]. The first unambiguous detection of an intrinsic field at Mars was achieved by the Mars Global Surveyor (MGS) mission [98Acu]. In contrast to other magnetic planets, the Martian field is lacking a strong dynamo component. Instead, the spectrum is dominated by components of degree larger than 10. The field strength varies between ±200 nT along the mapping orbit at 400 km height above the surface, the distance of the mapping orbit, and between ±1500 nT at the initial aerobreaking orbit with 100 km height. It has been concluded that the Martian crust must be about 10 times more intensely magnetized than the Earth's crust [02Vor]. Figure 1 shows the three components of the magnetic field at 400 ± 35 km height. The anomalies are clearly concentrated in the southern hemisphere of Mars, the surface of which is approximately 1 Ga younger than that of the southern hemisphere (see Section 4.2.3.5.1). The remnant magnetization of the Martian crust implies that Mars had a strong planetary field in the past. From the absence of magnetization in the Hellas basin it has been concluded that the planetary field was gone by the time of formation of the basin, a few hundred million years after formation of the planet [98Acu], [04Con]. This conclusion is widely but not unanimously accepted. Models of the magnetic of Mars predicted an early dynamo [83Ste, 90Sch]. The dynamo ceased to operate when the temperature difference between the core and the mantle became too small to drive convection and dynamo action in the core. The models predict a dynamo for roughly the first billion years of Martian history.

4.2.3.8.2.4 Moon

The Moon does not have a dipole field at present but large parts of the crust show remnant magnetization as shown in Figure 2 which is based on data from the US Lunar Prospector mission [07Mit]. The magnitude of the magnetization reaches values of up to 250 nT, much smaller than the magnetization of the Martian and the Earth's crust. The map suggests that the major impact basins show no crustal magnetization but some areas antipodal to the impact basins show a relatively strong field. This is particularly true for the Imbrium basin and to a lesser extent Mare Orientale. It has been suggested – e.g., [91Hoo] – that, therefore, the remnant magnetization is related to the impacts event although the magnetization occurs at antipodal sites [88Lin]. One model suggests that an impact-generated plasma cloud may sweep up the ambient magnetic field and converge at the antipodes where the field strength would then be large. The crustal rock shocked by the impact would then be magnetized by shock magnetization [83Cis].

4.2.3.8.2.5 Galilean satellites

The magnetometer onboard the Galileo spacecraft has measured magnetic signals at Europa, Ganymede and Callisto. For a review see [04Kiv]. The spacecraft failed to detect a magnetic signal at Io that could be attributed to an internal field of that satellite [97Khu]. Absence of a magnetic field at Io was predicted by [95Wie] who argued that heat production in Io's mantle by tidal dissipation was so dominant that little

heat was removed from the core. The core would therefore be entirely fluid and stably stratified with respect to thermal convection and thermal and chemical buoyancy would not be available to drive a dynamo. The magnetic signals detected at Europa and Callisto varied periodically along their orbits around Jupiter which was interpreted as evidence for electromagnetic induction [97Kiv]. The orbits of the satellites lie within the magnetosphere of the planet. It is widely accepted that the fields are induced in (salty) oceans underneath tens to hundred kilometre thick ice shells by the time varying magnetic flux of Jupiter's field. The signals measured at Ganymede, however, were interpreted as being due to a dipole field generated in the core of the satellite. The surface equatorial field strength is 719 nT and the dipole axis is tilted by 176° with respect to the rotation axis [02Kiv]. The dipole is rotated 24° toward the trailing hemisphere from the Jupiter-facing meridian plane. There is evidence for a smaller induced field in addition to the main field [02Kiv] but it is also possible that the signal is due to a quadrupole component of the main field.

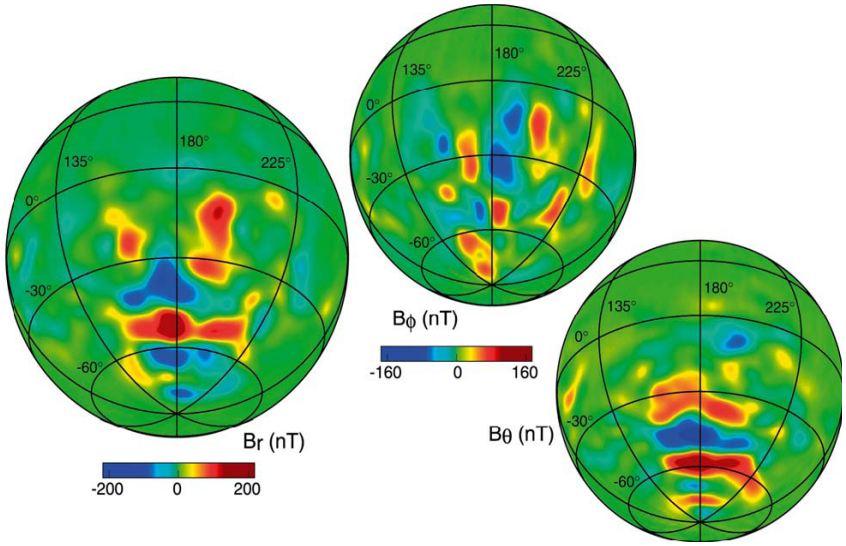

Fig. 1. (see color-picture part, page 625) Orthographic projections of the three components of the magnetic field (B_r , B_θ , B_Φ) at a nominal 400 km mapping orbit altitude, viewed from 30 deg S and 180 deg East longitude (from [04Con]). © Springer Verlag

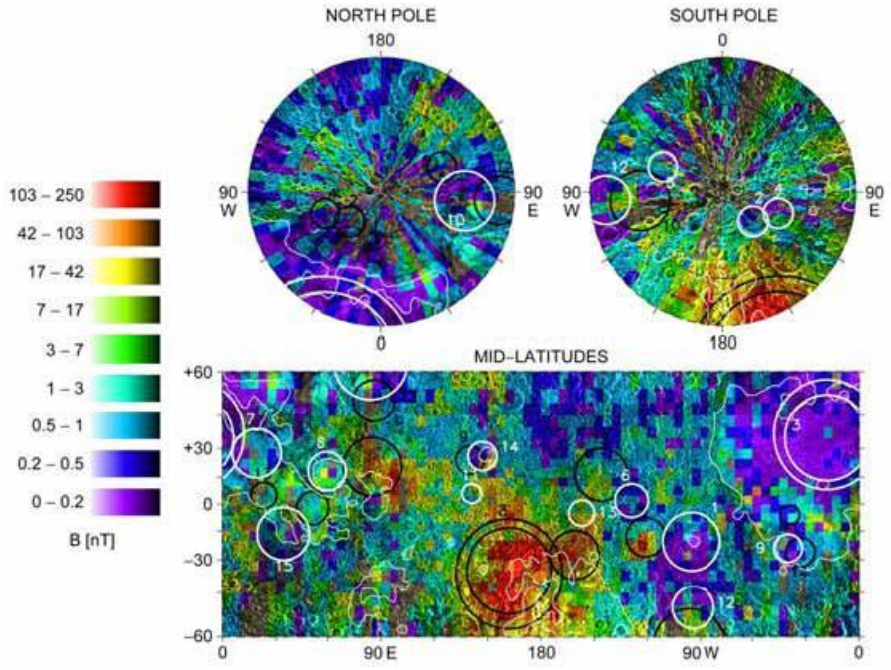

Fig. 2. (see color-picture part, page 625) Magnetic field at the surface of the Moon measured by the electron refelction experiment on Lunar Prospector in orthographic projection (from [07Mit]). The white circles indicate major impact basins and the black circles their antipodal regions. © American Geophysical Union

4.2.3.8.3 References for 4.2.3.8

74Nes Ness, N.F., et al.: Science **183** (1974) 130.
75Run Runcorn, S.K.: Nature **253** (1975) 701.
83Cis Cisowski, S.M., et al.: J. Geophys. Res. Suppl. **88** (1983) A691.
83Ste Stevenson, D.J., et al.: Icarus **54** (1983) 466.
87Phi Phillips, J.L., Russel, C.T.: J. Geophys. Res. **92** (1987) 2253.
88Lin Lin, R.P., et al.: Icarus **74** (1988) 529.
89Rie Riedler, W., et al.: Nature **341** (1989) 604.
90Sch Schubert, G., Spohn, T.: J. Geophys. Res. **95** (1990) 104.
91Hoo Hood, L.L., Huang, Z.: J. Geophys. Res. **96** (1991) 9837.
95Wie Wienbruch, U., Spohn, T.: Planet. Space. Sci. **43** (1995) 1045.
97Khu Khurana, K.K., et al.: Geophys. Res. Lett. **24**, (1997) 2391.
97Kiv Kivelson, M.G., et al.: Geophys. Res. Lett. **24** (1997) 2155.
98Acu Acuña, M.H., et al.: Science **279** (1998) 1676.
00Pur Purucker, M., et al.: Geophys. Res. Lett. **27** (2000) 2449.
02Kiv Kivelson, M.G., et al.: Icarus **157** (2002) 507.
02Vor Voorhies, C.V., et al.: J. Geophys. Res. **107** (E6) (2002).
04Con Connerney, J.E.P., et al.: Space Science Revs. **111** (1-2) (2004) 1.
04Kiv Kivelson, M.G., et al.: Magnetospheric Interactions with Satellites In: Jupiter. The Planet, Satellites and Magnetosphere, Cambridge University Press (2004) 513.
04Sta Stanley, S., et al.: Earth Planet. Sci. Lett. **234** (2004) 27.
06Chr Christensen, U.R., Aubert, J.: Geophys. J. Int. **166** (2006) 97.
07Bre Breuer, D., Moore, W.B.: Dynamics and Thermal History of the Terrestrial Planets, the Moon, and Io In: Planets and Moons, Treatise on Geophysics 10 Elsevier (2007) 299.
07Bus Busse, F.H., Simitev, R.: Planetary Dynamos In: Planets and Moons, Treatise on Geophysics 10 Elsevier (2007) 281.
07Chr Christensen, U.R., Wicht, J.: Numerical Dynamo Simulations, In : Core Dynamics, Treatise on Geophysics 8 Elsevier (2007) 245.
07Con Connerney, J.E.P.: Planetary Magnetism In: Planets and Moons, Treatise on Geophysics 10 Elsevier (2007) 243.
07Jon Jones, C.A.: Thermal and Compositional Convection in the Outer Core, In: Core Dynamics, Treatise on Geophysics 8 Elsevier (2007) 131.
07Mit Mitchell, D.L. et al.: J. Geophys. Res. **112(E6)** (2002) E01002.
07Rob Roberts, P.H.: Theory of the Geodynamo, In: Core Dynamics, Treatise on Geophysics 8 Elsevier (2007) 131.
08Wei Weiss, B.P., et al.: Science **322** (2008) 713.
09Uno Uno, H. et al.: Earth Planet. Sci. Lett, in press